ON THE EVOLUTIONARY STATE OF BETA CEPHEI STARS

Richard Stothers

Goddard Institute for Space Studies
National Aeronautics and Space Administration
New York, New York

[redacted]

ABSTRACT

An attempt is made to explain the β Cephei variables as non-rotating stars undergoing radial oscillations, on the basis of their relatively low observed rotational velocities and the period analyses by van Hoof. Arguments based on the central condensation and on the time scale of evolution vis-à-vis their observed numbers indicate that these B0.5 - B2 giants are in the hydrogen-burning phase. Model sequences are constructed for stars of 15 and 20 $M_\odot$ to the end of hydrogen-burning. The pulsational characteristics are then obtained by perturbing the stable models in the usual adiabatic approximation. Since the pulsational amplitude is greatest in the outer envelope, where the effective polytropic index is rapidly varying, it is shown that previous arguments based on polytropic models are liable to considerable error. Indeed, at some central hydrogen abundance which is higher for the lower masses, the periods and their ratios seem to be accounted for. Ideally, these quantities imply a unique mass and mean molecular weight for each observed star on the H-R diagram, but comparison of theory and observation gives at present merely a mass range of 10 - 20 $M_\odot$ and probably a "normal" chemical composition. At any rate, the hypothesis of evolution of main sequence O9 - B1 stars across

the instability strip seems to be correct. Uncertainties in the semiconvective theory of massive stars would appear to be irrelevant, since the quasi-stable zone has almost no effect on the pulsational eigenfrequencies. Theoretical and observational arguments indicate that the effects of rotation and mass loss will be small. The period-luminosity relation, observed luminosity classes, and location of the Trumpler turn-off in clusters tend to confirm our prediction that the β Cephei stars of lower mass fall closer to the initial main sequence. The Wolf-Rayet objects form an apparent extension of the instability strip to higher masses (O stars).

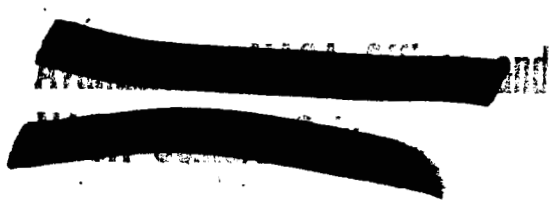

I. INTRODUCTION

The β Cephei stars are a group of short-period, pulsating variables. They form a well-defined sequence on the H-R diagram, running closely parallel to, although somewhat steeper than the main sequence at B0.5 - B2 and having luminosity classes III and IV. They obey a period-luminosity law, with periods ranging from 3.3 to 7 hours (toward higher luminosities). The observational data on the β Cephei stars, also called β Canis Majoris variables, have been summarized by Struve (1955b). There are now 18 or so known members of this group (van Hoof 1962e).

Since some of the β Cephei stars exhibit a beat phenomenon, caused by two nearly equal periods and appearing only in those members of the group with the highest projected rotational velocities (30 to 60 km/sec), Ledoux (1951, 1958) suggested that the instability was caused by rotation, and furthermore that it was probably manifested by non-radial oscillations. Basing their conclusions on crude interior models and only a rough notion of the mean densities of β Cephei stars, Ledoux and Walraven (1958) tried to show that the period-density relation calculated on the basis of radial oscillations was in conflict with the observations. More recently Gurm (1963) considered radial oscillations of a

main-sequence B1 star of 10 $M_\odot$ (Kushwaha 1957) and came to the same conclusion. Adopting the concept of non-radial oscillations and a suggestion by Chandrasekhar and Lebovitz (1962), Böhm-Vitense (1963) showed that the degree of period commensurability could be explained by the observed rotational velocities and vice versa, if the β Cephei stars were observed pole-on. She used the latter condition to explain the relatively small number of β Cephei stars among early B giants. However, her conclusions were based on idealized polytropic models of rotating stars from Schwarzschild (1958) and only a rough application of results from the Chandrasekhar-Lebovitz theory of non-radial oscillations of rotating fluid spheres.

Since rotation is not always observed in the β Cephei stars, and is in any case small in comparison with 100 to 200 km/sec for main-sequence and giant stars of the same spectral type (McNamara and Hansen 1961), it seems worthwhile, still, to consider the variables as non-rotating stars undergoing radial oscillations. Struve (1955b) has emphasized that many of the β Cephei stars are relatively simple variable stars, completely analogous to other variables that are believed to be in purely radial oscillation. In fact, van Hoof (1962e) has shown that many of the observed features of the β Cephei phenomenon may be explained by the interference of several simultaneously excited modes of

radial oscillation.

It is the purpose of this paper to determine at which evolutionary stage massive stars become β Cephei variables, and to see whether the relevant observations may be explained on the assumption of radial pulsation.

II. PRELIMINARY EVOLUTIONARY CONSIDERATIONS

From a discussion by Schmalberger (1960), the β Cephei stars lie on the H-R diagram near the locus of models at the end of hydrogen-burning. This locus is defined by the first turn back toward the main sequence. Thus the β Cephei stars appear to have evolved from main sequence O9 - B1 stars. Since calculated luminosities for models of upper main sequence stars are fairly accurate, we may use the observed period-absolute magnitude relation to obtain the period-mass relation: Π (hours) = 0.35 $M/M_{\odot}$, where the mass range is roughly 10 - 20 $M_{\odot}$. The major uncertainty lies in the bolometric corrections to the observed magnitudes. There are no observed masses of these stars.

If the β Cephei stars are indeed situated along the locus of secondary contraction, then some ambiguity arises because the evolutionary track for models of massive stars swings back quickly

to the right after the brief turnback, forming an S-shaped curve. The luminosity becomes only slightly higher, but the internal structure is grossly changed from a core burning configuration to a contracting core with a surrounding, hydrogen-burning shell (Sakashita, Ôno, and Hayashi 1959; Hayashi and Cameron 1962; Stothers 1963 and 1964, hereafter called "Paper I" and "Paper II", respectively). The contraction phase was suggested by Reddish (Discussion, Reddish and Sweet 1960).

Two lines of evidence point strongly to the former configuration for the β Cephei stars. The first line of evidence is based on the observed statistics of these stars. If our sample of 18 stars (van Hoof 1962e) is complete within a kiloparsec radius around the sun, in a Galaxy of effective R = 10 kiloparsecs, and if there is a maximum of 1×10^5 O - B2 stars in the Galaxy, then the number ratio of β Cephei stars to all O - B2 stars will be less than 1/50. In fact, McNamara and Hansen (1961) have obtained the ratio 1/9. Now according to Hayashi and Cameron (1962), the gravitational (core) contraction phase of a star of 15.6 $M_\odot$ is 1/200 as long as the hydrogen-burning phase. If hydrogen-exhaustion is counted with the gravitational contraction phase, the ratio becomes 1/80. These ratios are far larger than the observed ones.

The second line of evidence concerns the period ratios,

according to the work of van Hoof and the results to be derived in this paper. During the hydrogen-burning phase, the calculated and observed period ratios agree at some characteristic central hydrogen abundance, dependent on the stellar mass. However, increasing central condensation leads to more and more discrepant values for these ratios.

Hence we conclude that we must seek models for the β Cephei stars in the hydrogen-burning phase of evolution.

III. STABLE MODELS

a) Basic Physics

The general structure assumed for models of massive stars has been outlined in Paper I. Here we adopt the same assumptions, notations, and equations as before. The adopted masses are 15 and 20 $M_\odot$, since at 10 $M_\odot$ electron scattering is no longer a good approximation to the opacity throughout the star. The initial composition is again taken to be

$$X_e = 0.70,\ Y_e = 0.27,\ Z_e = 0.03,\ X_{CNO} = Z_e/2. \quad (1)$$

The parameters in the formula for nuclear energy generation are, in the present case,

$T_c < 37 \times 10^6$ $\quad \nu = 16$ $\quad \log \varepsilon_o = -114.1$

$T_c > 37 \times 10^6$ $\quad \nu = 15$ $\quad \log \varepsilon_o = -106.6.$ (2)

b) Integration of Equilibrium Equations

The construction of models proceeds in the manner outlined in Paper I. However, the fitting was accomplished completely automatically by the computer, as follows. We denote the envelope eigenvalue by α. Thus for the initial model $\alpha = \log C$, and for the inhomogeneous models $\alpha = \lambda$ (the composition exponent). The integrations of the outer radiative Zone I and the assumed radiative intermediate Zone III are performed as in Paper I, and then smoothly continued into Zone IV, the convective core, when $(n + 1)_{ad} = (n + 1)_{rad}$. Care must be exercised in selecting the proper fitting point, since $(n + 1)_{ad} = (n + 1)_{rad}$ at the semiconvective zone, too. Once inside the core, the inward integrations are tested on the U-q plane at each point. If $U > 3$ or $dU/dq > 0$, the current value of q (say, $q_>$) is noted, and the whole integration is begun again from the surface (for the initial model) or from q_1 (for the inhomogeneous models) with a revised estimate of α based on the smallness of $q_>$. When $q_>$ is less than a suitably small prechosen value, an extrapolated

value of β_c is obtained.

The integration method is now altered as follows. From the last trial integration a fitting point is selected just inside the core; the value of $\beta = \beta_f$ is noted. Now two inward integrations are performed for α and $\alpha + \Delta\alpha$, in to β_f. Here the values of U and V are noted. Similarly, two outward integrations from the center are performed for β_c and $\beta_c + \Delta\beta_c$. From the two inward integrations we may form $\delta U/\delta\alpha$ and $\delta V/\delta\alpha$, and from the two outward integrations $\delta U/\delta\beta_c$ and $\delta V/\delta\beta_c$, all evaluated at β_f. We obtain improved values of α and β_c by using the increments $\Delta\alpha$ and $\Delta\beta_c$ derived from a solution of the two simultaneous equations,

$$U_{out} - U_{in} = \frac{\delta U}{\delta\alpha}\Delta\alpha - \frac{\delta U}{\delta\beta_c}\Delta\beta_c$$
$$V_{out} - V_{in} = \frac{\delta V}{\delta\alpha}\Delta\alpha - \frac{\delta V}{\delta\beta_c}\Delta\beta_c . \qquad (3)$$

This method is iterated until $\Delta\alpha$ and $\Delta\beta_c$ are suitably small.

When Zones I, III, and IV become properly fitted in U, V, and β, the semiconvective Zone II is integrated and fitted to Zone III as shown in Paper I.

c) Results for Stable Models

Table 1 contains the essential results for evolutionary sequences of six models obtained for stars of 15 and 20 $M_\odot$.

Comparison may be made with the analogous sequence calculated for 30 $M_\odot$ in Paper I. It should be noted that in this paper the adopted values of $L_\odot$ and $R_\odot$ are those of Allen (1963), whereas in Papers I and II Chandrasekhar's (1939) values were used. In all comparisons with other work, we shall renormalize luminosities and radii to Allen's values whenever necessary.

Apart from the increasing importance of the semiconvective zone from 15 to 30 $M_\odot$, the only other point worthy of special mention is that the initial decrease of central density for stars of intermediate and high mass becomes negligible or even vanishes for very massive stars, at some mass between 20 and 30 $M_\odot$ (cf. also Henyey, LeLevier, and Levée 1959). It seems that the nuclear energy generation is not quite sufficient to expand the central regions against their slow gravitational contraction. This would be due to the lower value of ν, which leads to a less steep gradient of temperature and hence of pressure.

IV. PULSATING MODELS

a) Pulsation Equation

The equation describing small, radial adiabatic pulsations of a spherically symmetric fluid may be written

$$\frac{\partial^2 \xi}{\partial r^2} + \frac{\partial \xi}{\partial r}\left[\frac{2}{r} + \frac{1}{\Gamma_1 P}\frac{\partial}{\partial r}(\Gamma_1 P)\right] + \xi\left[\frac{\sigma^2 r\rho + 4g\rho}{\Gamma_1 P r} - \frac{2}{r^2} + \frac{2}{\Gamma_1 P r}\frac{\partial}{\partial r}(\Gamma_1 P)\right] = 0, \quad (4)$$

where ξ is the radial displacement, $\sigma/2\pi = \Pi^{-1}$ the frequency and Π the period of oscillation. We have also the adiabatic exponent

$$\Gamma_1 = \beta + \frac{(4-3\beta)^2(\gamma-1)}{\beta + 12(\gamma-1)(1-\beta)} \quad (5)$$

for a mixture of perfect gas and radiation (Chandrasekhar 1939). Equation (4) is the equation derived by Ledoux (1939) if the relative amplitude $\delta r/r$ is introduced in place of $\xi = \delta r$. Since the coefficients of the pulsation equation have singularities at the surface and center, we have the following boundary conditions:

$$\delta P = -\Gamma_1 P\left(2\frac{\xi}{r} + \frac{\partial \xi}{\partial r}\right) = 0, \qquad (r = R)$$
$$\delta r = \xi = 0. \qquad (r = 0) \quad (6)$$

It will be convenient to evaluate an explicit expression for $\partial(\Gamma_1 P)/\partial r$. Since the ionization zones of hydrogen and helium are of negligible extent in massive stars, we may take $\gamma = 5/3$ throughout the whole star. Then we obtain from equation (5)

$$\delta\Gamma_1 = \frac{7\Gamma_1 - 8 - 2\beta}{8-7}\,\delta\beta, \quad (7)$$

and from the equation of state

$$d\beta = (1-\beta)(d\ln P - 4\, d\ln T). \tag{8}$$

With the help of the homology invariants $V = -\, d\ln P/d\ln r$ and $n + 1 = d\ln P/d\ln T$, we obtain the desired expression

$$\frac{1}{\Gamma_1 P}\frac{\partial}{\partial r}(\Gamma_1 P) = -\frac{V}{r}(1+b), \tag{9}$$

where

$$b = \frac{(1-\beta)(n-3)}{B(n+1)}, \qquad B = \frac{\Gamma_1(8-7\beta)}{7\Gamma_1 - 8 - 2\beta}. \tag{10}$$

Introducing equation (9), V, and $\beta P = k\rho T/\mu H$ into equation (4), we rewrite the pulsation equation as

$$\frac{\partial^2 \xi}{\partial r^2} + \frac{\partial \xi}{\partial r}\left[\frac{2}{r} - \frac{V}{r}(1+b)\right] + \xi\left[\frac{\sigma^2}{G}\frac{V r}{\Gamma_1 M(r)} - \frac{2}{r^2} - \frac{2V}{r^2}\left(1+b-\frac{2}{\Gamma_1}\right)\right] = 0. \tag{11}$$

This is the final form of the pulsation equation, taking radiation pressure exactly into account. In the case of no radiation pressure ($1 - \beta = b = 0$), $\Gamma_1 = \gamma$ and equation (11) reduces to the equation used by Stothers and Schwarzschild (1961).

In terms of the non-dimensional envelope variables defined in Paper I equation (11) becomes

$$\frac{\partial^2 \xi}{\partial x^2} + \frac{\partial \xi}{\partial x}\left[\frac{2}{x} - \frac{V}{x}(1+b)\right] + \xi\left[\omega^2 \frac{V x}{\Gamma_1 q} - \frac{2}{x^2} - \frac{2V}{x}\left(1+b-\frac{2}{\Gamma_1}\right)\right] = 0, \tag{12}$$

where

$$\omega^2 = \sigma^2 \frac{R^3}{GM} \tag{13}$$

is the eigenvalue of the problem. For homologous stars ω^2 is constant, so that we obtain the familiar relation $\Pi \sqrt{\rho}$ = const.

In the core of the star, the pulsation equation may be written as equation (12) with the envelope variables simply replaced by the starred core variables of Paper I. In this case the eigenvalue is

$$\omega^{*2} = \sigma^2 \frac{r_0^3}{GM_0} = \omega^2 \frac{\beta_c \bar{\rho}}{3\rho_c} . \tag{14}$$

b) Starting Series

Because of the singularity at the stellar surface, the solution of the pulsation equation must be expanded in a power series around r = R. To do this, we first introduce the zero surface expansions from Paper I into equation (12). We note the necessary expressions for the homology invariants:

$$U = 0, \quad V = \frac{n+1}{1-x}, \quad n+1 = 4. \tag{15}$$

Then equation (12) becomes, near the surface,

$$x^2(x-1)\frac{\partial^2 \xi}{\partial x^2} + 2x(x+1)\frac{\partial \xi}{\partial x} - (\omega_s^2 x^3 + 2x - \gamma_s)\,\xi = 0, \tag{16}$$

where

$$\omega_s^2 = \frac{4}{\Gamma_1^0}\,\omega^2, \qquad \gamma_s = 2 - 8\left(\frac{2-\Gamma_1^0}{\Gamma_1^0}\right), \tag{17}$$

and $\Gamma_1^0 = \Gamma_1(\beta_0)$. We now expand ξ in a power series in terms of the small (negative) quantity $x - 1$:

$$\xi = \sum_{k=0}^{\infty} \xi_k(\omega^2)\,(x-1)^k. \tag{18}$$

Introduction of this expression into equation (16) yields the following recursion relation among the coefficients $\xi_k(\omega^2)$:

$$\begin{aligned} k(k+3)\,\xi_k = {} & \omega_s^2\,\xi_{k-4} + 3\omega_s^2\,\xi_{k-3} + (3\omega_s^2 + 3k - k^2)\,\xi_{k-2} \\ & + (\omega_s^2 - \gamma_s + 4 - 2k^2)\,\xi_{k-1}, \end{aligned} \tag{19}$$

where $\xi_{-1} = \xi_{-2} = \xi_{-3} = 0$. Note that the magnitudes of the coefficients are relative to the magnitude of ξ_0. Normalizing the amplitude at the surface ($x = 1$), we have that $\xi_0 = 1$.

The solution of the pulsation equation is similarly expanded in a power series around $r = 0$. From the center expansions of Paper I, we note that V is a quantity of second order and $\beta \approx \beta_c$, so that

$$U = 0, \quad V = 0, \quad n+1 = (n+1)_c. \tag{20}$$

Then equation (12) becomes, near the center,

$$x^{*2} \frac{\partial^2 \xi}{\partial x^{*2}} + 2x^* \frac{\partial \xi}{\partial x^*} - 2\xi = 0, \tag{21}$$

which is independent of β_c and ω^{*2}. The solution is simply

$$\xi = \xi_o^* x^*. \tag{22}$$

c) Integration of Pulsation Equation

It is convenient to split the second-order differential equation (12) into two coupled, first-order equations with the help of the auxiliary quantity $\psi = \partial\xi/\partial x$. By a suitable choice of independent variables in place of x for the various regions of the star, these two equations may be accurately integrated rather close to the stellar center. Since the solution for arbitrary ω^2 will, in general, diverge as the center is approached, the following procedure was used to obtain the correct eigenvalue that makes ξ and ψ small near the center. For each mode, two trial values of ω^2 are guessed, and integrations are performed in both cases down to a small, prechosen value of q (say q_e). Then an improved value of ω^2 is calculated from the magnitude and sign of ψ at q_e. The procedure is iterated until $\psi \approx 0$ at q_e.

Improvement is now obtained by the same method that was used

in calculating the stable models (Section IIIb). We fit the core and envelope solutions at β_f, using $\partial\xi/\partial\beta$ and $\partial^2\xi/\partial\beta^2$ as fitting parameters. The inward and outward values of these parameters are normalized by the ratio of the inward and outward values of ξ at β_f. An alternative procedure is to use equation (14) for ω^{*2} directly from the trial value of ω^2 and our knowledge of $\bar{\rho}$ and ρ_c from the stable model. Then only one equation of (3) has to be used to obtain improved values of ω^2 and hence of ω^{*2}. We note that, besides β_c, ω^{*2} depends on ω^2 only through X_c and t_4/t_4^* (from the stable model).

d) Results for Pulsating Models

The pulsational characteristics of massive stars are collected in Table 2. It is to be noted that, since ω^2 and ω^{*2} are independent of the nuclear energy generation and hence of the stellar radius, so are $\rho_c/\bar{\rho}$ and the period ratios. They depend only on β_c and the total luminosity, apart from the age and initial chemical composition. The period-root-mean-density relation is given by $Q = \Pi\sqrt{(\bar{\rho}/\bar{\rho}_\odot)}$. It does not change much from mass to mass, for models at the same evolutionary state. The same statement is true for $\rho_c/\bar{\rho}$ and the period ratios.

We note that ω^2 does not depend very strongly on the central

condensation. For instance, between models 1 and 2 for 15 $M_\odot$, $\rho_c/\bar{\rho}$ doubles. Likewise, between models 3 and 5 it doubles again. However, the change of ω^2 in the latter case is much smaller than in the former. The reason is that ω^2 depends on the rate of decrease of ξ, which drops rapidly in the outer envelope, and therefore is insensitive to the precise interior conditions. Figure 1 shows this in the case of the five calculated modes for model 4 of 15 $M_\odot$. Since ξ is determined chiefly by the structure of the envelope and hence by the total luminosity, so is ω^2. Now we note that the luminosity increases much less between models 3 and 5 than between models 1 and 2.

Tables 1 and 2 also show that ω_o^2 and the period ratios decrease with β and Γ_1. This may be seen by comparing the initial models for the three masses. The effect is similar to that found in the standard model (Ledoux and Walraven 1958). However, detailed comparisons using the standard model appear to be very misleading, because the effective polytropic index throughout the envelope actually drops far below n = 3 (see Figure 2). This leads to greatly different values of the pulsational quantities. In the last column of Table 3, Schwarzschild's (1941) results on the standard model are listed. We see that our values of Q_o are even larger than Q_o of the standard model, which Ledoux and Walraven

found to be in excess of their "observed" value for the β Cephei stars, $Q_o = 0.027$. However, the values they used for the radii of these stars were too large.

Gurm (1963) calculated the pulsational eigenvalues for Kushwaha's (1957) initial main sequence model of 10 $M_\odot$ and $X_e = 0.90$, and found $\Pi_o = 2.12$ hours. Since we see from Table 2 that the period more than doubles along the evolutionary track of massive stars, his conclusion that our present theory of stars on the upper main sequence seems inadequate, because of the period disagreement, appears to be unwarranted. In fact, as we shall see in Section VIa, the periods (but not their ratios) may be considerably altered through small changes in the chemical composition. Moreover, we have seen that arguments based on changing the central condensation of models do not lead very far, since Table 3 shows that even the standard model gives a fair representation of $\rho_c/\bar{\rho}$. Finally, a gradient of effective polytropic index, such as occurs in the models calculated here, seems necessary to yield correct values of $\rho_c/\bar{\rho}$ and ω_o^2.

Reddish and Sweet (1960) interpreted Struve's tentative suggestion of a secular period change in β Cephei in terms of the expanding radius during hydrogen-burning. Their rough result that the rate of increase is an order of magnitude smaller than that required by observations is confirmed by our detailed models. This is a further indication that beat phenomena and slow period changes in β Cephei stars may be explained by interacting modes.

V. DATA ON THE BETA CEPHEI STARS

In Table 4 the results of van Hoof's analyses of the light curves of five β Cephei stars are presented. A similar analysis of ξ_1 Canis Majoris is not presented, since it was essentially an interpolation (van Hoof 1963). However, these stars are representative of all the β Cephei stars, in that they include a broad range of periods, rotational velocities, and velocity amplitudes. The data of Table 4 were used to interpolate the models presented in Table 3. All the period ratios agreed; therefore we listed only the adopted Π_1/Π_o for each mass.

To plot the observational data for β Cephei stars on the theoretical H-R diagram, we have used the list given by van Hoof (1962e) and the relations between spectrum, effective temperature, and bolometric correction given by Harris (1963). Harris's bolometric corrections were used for all luminosity classes (II - IV). The luminosities were normalized by using $M_{bol} = +4.72$ for the sun (Allen 1963). The resulting values of luminosity and effective temperature are not very different from those obtained by Schmalberger (1960).

The evolutionary tracks on Figure 3 came from Papers I, II, and the present paper for 15 - 20 - 30 $M_\odot$, and from Henyey *et al.*

(1959) for 11 - 20 $M_\odot$. Crosses denote the interpolated models of Table 3.

It is clear from Figure 3, as well as Table 3, that the locus of constant period ratios is not the locus of secondary contraction. We shall not concern ourselves that the constant-ratio strip falls to the left of the observed β Cephei strip and that the periods do not quite agree; both of these discrepancies may easily be removed by a change in the radius, accomplishable in several ways, as shown in the next section. It is therefore of somewhat academic interest to recall that Struve (1955a) had earlier proposed evolution of stars up the β Cephei strip, in the absence of any detailed models at the time.

VI. EFFECT OF CHANGING PHYSICAL PARAMETERS

a) Chemical Composition

In general, a change in the initial chemical composition of a star whose opacity is dominated by electron scattering will shift its evolutionary track along a diagonal line almost parallel to the initial main sequence in the H-R diagram. For, since $L \sim \mu_e^4$ and $R \sim \mu_e$, we have that $T_e \sim \mu_e^{1/2}$.

If we assume that all the β Cephei stars have the same mass and pulsate at the same evolutionary stage, but have different initial chemical compositions, then $\Pi \sim R^{3/2} \sim \mu_e^{3/2}$. Since Π is observed to vary by a factor of 2, we must conclude that X_e also varies by at least the same factor. This conclusion seems to be unjustified by observations of the upper main sequence. Moreover, the period ratios will be different at the same evolutionary stage, in contradiction of the observed rough constancy of these ratios. Finally, the variation in X_e necessary to produce the observed variation in luminosity is much more than a factor of 2.

The last argument would also rule out the possibility of pulsation at differing evolutionary stages, even though supplementary calculations indicate that the constant-ratio strip on the H-R diagram for stars of the same mass but differing initial chemical composition falls in the same way as in Figure 3. The reason for the similar position of the strip is that ω_o^2 and the period ratios at the same evolutionary stage (l_c) are smaller for stars of lower X_e (and hence higher luminosity).

If, however, we assume with Schmalberger (1960) that all the β Cephei stars fall along the locus of secondary contraction ($X_c \approx 0.03$) on the H-R diagram, we can compute the necessary initial chemical composition for each mass on the basis of constancy

of the period ratios. From Table 3 the model for 30 $M_\odot$ with $X_e = 0.70$ almost fulfils the criteria. Using it as a standard, we invoke homology arguments to calculate X_e for other masses. From Paper I, as long as β_c is not too low, the dimensionless structure of the star is specified only by the parameters A and C at a given evolutionary stage (l_c), since the variable j may be replaced by $l^{0.285}$ (Schwarzschild 1958). Then, holding A constant, we calculate that X_e must be 0.46 and 0.32, for 20 $M_\odot$ and 15 $M_\odot$, respectively. Since the pulsational eigenvalues and hence period ratios depend only on the dimensionless structure of the star, these values of X_e seem to be necessary for the hypothesis of secondary contraction. They are unrealistically low, and should be lower still because the mass at which $X_e = 0.70$ is actually greater than 30 $M_\odot$, and because the decreased values of X_e imply an increased luminosity. Therefore, to give agreement with the observed luminosities, even smaller masses and hence lower X_e would have to be taken. Moreover, there is no reason to believe that the calculated periods would agree with the observations. In any case, it is difficult to see why β Cephei stars of lower mass should have lower initial hydrogen abundances.

Ideally, if the β Cephei strip were sufficiently well defined observationally, the stellar masses and chemical compositions could

be determined with greater accuracy. For a given model, specified by M and μ_e, the evolutionary track crosses the strip on the H-R diagram at a certain point, where both Π_o and the period ratios must agree with the observations. Since Π_o depends essentially on the stellar radius and the period ratios on the luminosity, the required model is therefore uniquely determined.

b) Nuclear Energy Generation

The radius of massive stars is essentially determined by the rate of nuclear energy generation. Since $\Pi \sim R^{3/2}$, it is clear that we may seek agreement with the observed periods by adjusting ε_o or X_{CNO}, as well as by changing μ_e (see previous subsection). To change Π_o of the model for 15 $M_\odot$ that best fits the observations of period ratios, from 3.7 to 5 days, we require an increase in ε_o or X_{CNO} by a factor of 45. Such an increase seems inadmissible. Moreover, the increase does not scale homologously with inverse mass but is constant, so that agreement with observations at 15 $M_\odot$ produces too great a Π_o at 20 $M_\odot$. It should also be recalled that changing R and hence the periods does not change the period ratios.

c) Opacity

The inability of a reasonable change in the nuclear energy generation rate to produce agreement with the observed periods will not be disastrous, however. In our models we neglected opacity sources other than electron scattering, and it is certain that bound-free absorption processes will contribute non-negligibly in the outer envelope. The model sequence for 20 $M_\odot$ with $X_e = 0.68$, computed by Henyey, LeLevier, and Levée (1959), included these processes, and the resulting evolutionary sequence lies on the H-R diagram parallel to our sequence at very nearly the same luminosity. It is, however, displaced to lower effective temperatures by an amount equivalent to a change in log $(R/R_\odot)$ equal to 0.06, after allowance for differences in X_e, X_{CNO}, and ϵ_o. This change is brought about almost directly by the opacity, since we have that $R \sim \kappa$, from a dimensional analysis of the equation of energy transport by radiation. The change produces an increase of Π_o from 5.2 to 6.4 days, more closely in agreement with observations.

The question arises whether inclusion of bound-free absorption will change the pulsational eigenvalues. Undoubtedly it will to some extent, but the ratios of the modes, especially those of the higher modes, should remain fairly constant, because they are nearly

independent of the radius. We recall that it is these ratios that essentially fix the β Cephei strip in the evolutionary H-R diagram.

It may easily be shown, however, that the inclusion of bound-free absorption, which has an increasing effect at lower masses, actually serves to offset the line of constant period ratios farther from the locus of secondary contraction. Its inclusion is roughly equivalent to increasing X in the electron scattering opacity. As discussed in Section VIa, the period ratios then also increase. Therefore, at lower masses, the model for which the ratios agree with observations lies closer to the initial main sequence. However, as stated above, the effect should be small.

d) Semiconvection

Since the extent of semiconvection in a star depends mainly on the luminosity, a lowering of the initial hydrogen abundance in stars of a given mass increases the amount of semiconvection, through the relation $L \sim \mu_e^4$. However, the semiconvective zone, as we have treated it, is unable to alter the pulsational eigenvalues to a perceptible degree, even in the last hydrogen-burning model of a star of 30 $M_\odot$. Hence uncertainties in the semiconvective theory will probably not be reflected in the pulsational

characteristics of massive stars. For determination of these characteristics, it is adequate merely to consider the intermediate zones as wholly radiative.

VII. DYNAMICAL EFFECTS

a) Rotation

Rotational effects should be small, since McNamara and Hansen (1961) have shown that the average equatorial velocity for β Cephei stars is only 22 km/sec. In addition, theoretical evidence exists that large rotation may inhibit pulsations (Steinitz 1964). However, the fact that somewhat higher rotational velocities are observed in the case of β Cephei stars exhibiting a beat phenomenon indicates that the presence of secondary periods may be due to the rotation. At any rate, the work of McNamara and Hansen (1961) and the summary by Struve (1955b) strengthen the case for purely radial oscillations in the slowly rotating β Cephei stars. In view of the observed period-luminosity relation and van Hoof's work, this statement probably holds true also for the more rapidly rotating stars.

b) Energizing Mechanisms

Schwarzschild and Härm (1959) have shown that upper main sequence stars become pulsationally unstable above about 60 $M_\odot$. At these masses Γ_1 approaches 4/3 because of the high radiation pressure, and nuclear reactions are able to supply enough energy to maintain the instability. Stars of lower mass should be pulsationally stable nuclear-wise, and explicit calculations by Gurm (1963) for 10 $M_\odot$ confirm this expectation.

Rotational energy is a second possible source for the pulsations. As evolution off the main sequence proceeds, the envelope expands and hence displays a lower rotational velocity. At the same time, the core is contracting and, in the absence of dissipative mechanisms, will rotate faster. Since the β Cephei stars as a group show rotational velocities far less than the velocities shown by stable stars of the same spectral and luminosity classes, possibly the angular momentum has been transferred to the core and used in energizing the pulsations. However, Figure 1 suggests that rotational energy of the core may not be a source for the pulsations since the pulsational amplitude here is less than 1 per cent of its value at the surface. It is partly for the same reason that nuclear energy fails as a source.

Further, as we have already mentioned, indirect theoretical

evidence shows that rotation of a star as a whole tends to inhibit pulsations (Steinitz 1964). In analogy with the cepheids, if the hydrogen or helium ionization zones are the source of the pulsations, then they originate in the atmosphere or not far below the photosphere. Atmospheric expulsion is indeed what is required to explain the beat phenomenon according to the theory of Struve and Odgers (Struve 1955b). If molecular dissociation is the cause of the instability, then some reasonably abundant molecule must be dissociating at temperatures typical of B0.5 - B2 giants.

c) Mass Loss

If the theory of Struve and Odgers (Struve 1955b) is correct, the β Cephei phenomenon may be explained by the ejection, deceleration, and subsequent infall of an atmosphere. In any case, it is to be expected that some mass will be lost (Sahade in Discussion, Reddish and Sweet 1960). We should like now to examine whether the β Cephei strip (or constant-ratio strip) is actually the evolutionary track of a star losing mass.

If the star remains chemically inhomogeneous, a constant-ratio line cannot be maintained since X_c along the line increases as the stellar mass is lower (Table 3). If, however, the incipient instability causes and then maintains complete mixing of the stellar material, a constant-ratio line might be maintained since

X_c (= X_e) decreases with the mass. For average values of M and L taken from Table 1, the lifetime of a star of initially 20 $M_\odot$ to reach 10 $M_\odot$ will be $\Delta\tau = E\,\Delta X\,\langle M\rangle/\langle L\rangle = 10^7$ years. Hence the mean rate of mass loss is 10^{-6} $M_\odot$/year; this rate might not be unreasonable.

Three arguments seem to rule out complete mixing, however. First, the mass would be forced to decrease with X_e as μ_e^{-2} in order to preserve constancy of the period ratios (see Section VIa). Second, since $L \sim \mu_e^4 M^3/(1 + X_e) \sim M/(1 + X_e)$, and both M and $1 + X_e$ decrease by about the same factor, L will not change very much, in contradiction to the observations. Third, complete mixing not only restores stars to the initial main sequence, but as hydrogen is consumed, it produces a track to the left. A compromise based on partial mixing may be ruled out by the same argument applied against the inhomogeneous case.

We conclude that theory predicts little mass loss, and in the absence of any direct observational evidence to the contrary, we have assumed that stars must therefore evolve across the instability strip. Since the strip is so narrow, the time scale of evolution across it must be small, and therefore the mass loss in any case will be small.

VIII. INTERPRETATION OF THE H-R DIAGRAM

We should now like to see whether the rapid drop in luminosity along the constant-ratio line is more compatible with the observations than the gentler drop occurring strictly along the locus of secondary contraction, as suggested by Schmalberger (1960). First, since no known β Cephei stars are members of a binary system, we have relied on the model calculations to place the mass limits at 10 and 20 $M_\odot$, roughly. Then our constant-ratio models predict a period-luminosity law $\Pi \sim L^{0.40}$ in this range. (Extrapolating from 15 $M_\odot$ to 10 $M_\odot$, we should actually have an exponent slightly less than 0.40.) Since Π will change by a roughly constant multiple for all model masses if the constants determining R are changed, the exponent 0.40 will remain unchanged for horizontal shifts of the evolutionary tracks in the H-R diagram. Now all the β Cephei stars taken together (van Hoof 1962e) yield a law $\Pi \sim L^{0.25}$. However, only four of them have accurately determined luminosities. These are members of the Scorpio-Centaurus cluster, and include θ Ophiuchus and β Crucis from Table 4. They yield the law $\Pi \sim L^{0.35}$. Good agreement is therefore found with the theoretical law.

Second, the luminosity class drops from II - III for the

variables of earliest spectral type (B0.5) to IV for those of latest spectral type (B2). This suggests that the β Cephei strip does indeed approach the main sequence closer than does the locus of secondary contraction, which should probably not show a drop, or at least a large one, in luminosity class. We note further that the magnitude difference between class IV and V stars attains a minimum at B2 (Arp 1958). From Figure 3 the constant-ratio strip, extrapolated, would run close to the initial main sequence at 10 $M_{\odot}$ (B2).

Third, observations of early-type clusters and associations indicate that the tip of the Trumpler turn-off, which by age arguments is believed to represent the point of secondary contraction, occurs at luminosity class III. For example, in I Geminorum the turn-off from the initial main sequence appears at B1 V and the tip of the turn-off at B1 III (Crawford, Limber, Mendoza, Schulte, Steinman, and Swihart 1955). This suggests that the B1 IV β Cephei stars would not have reached the end of hydrogen-burning.

The observed spectral (or mass) range of the β Cephei stars is remarkably well defined. One indication that the lower mass cutoff should occur near B2 is that our calculations show an intersection of the extrapolated constant-ratio strip with the main sequence near 10 $M_{\odot}$. Secondly, noting that the β Cephei stars

occur only among sharp-line (slowly rotating) early B stars, McNamara and Hansen (1961) ascribe the cutoff to increasing rotational velocities among the late-type B stars. (This increase is observed in both luminosity classes V and III [Allen 1963].) Thus observations, as well as theory, indicate that large rotation tends to inhibit pulsational instability.

An unfruitful suggestion regarding the upper limit to the mass is that semiconvection starts to become important in stellar envelopes at about 20 $M_{\odot}$. Although convection tends to damp pulsations, the semiconvective zone is too ineffective and lies too deep for this purpose (see Fig. 1).

Observational evidence exists, however, for the continuation of instability up to the highest masses. But in the case of the O giants, the instability manifests itself in the Wolf-Rayet phenomenon. Westerlund (1961) and Westerlund and Smith (1963) have shown that in the H-R diagrams of O clusters in the Large Magellanic Cloud, the Wolf-Rayet stars appear invariably at the tip of the Trumpler turn-off. These authors suggest that the masses of the Wolf-Rayet stars lie between 20 and 60 $M_{\odot}$, which is what we require to explain them as an "extension" of the β Cephei strip, now occurring close to the locus of secondary contraction.

Sahade (1962) gives a table of computed masses for some of

the galactic Wolf-Rayet stars. Although they appear to be less massive than their OB companions, the three luminosity classes given for the companions are all class I. Hence we expect these companions to be more massive, since they have presumably evolved further (past the Wolf-Rayet phase of pseudo-class O III).

Finally, in an analysis of Wolf-Rayet spectra Smith (1955) has reported variability of emission line intensities on a time scale of a few hours, in analogy with the Of stars (Oke 1954). We emphasize, however, that the observable form of the instability and probably the energizing mechanisms sustaining it are wholly different for the Wolf-Rayet and β Cephei stars. Why an apparent changeover should occur at B0 is unknown.

IX. CONCLUSION

It appears that radial pulsations of hydrogen-burning giants may be adequate to explain the observations of β Cephei stars. Non-radial or strictly atmospheric pulsations need not be invoked. However, the effect of rotation and possible mass loss cannot be definitely ascertained, although it is probable that they are small. In any case, theory cannot yet say why the β Cephei stars lie in the distinct range B0.5 - B2 III - IV, nor why only some stars in

this range become variable, nor what the sources maintaining several simultaneously excited modes may be.

A preliminary theoretical discussion of the β Cephei stars appeared in the author's doctoral dissertation, Harvard University (1963), which was supported in part by a Harvard scholarship during the first half of the academic year 1963 - 1964. Another part of the work reported in this paper was supported by an NAS-NRC Postdoctoral Resident Research Associateship under the National Aeronautics and Space Administration. It is a pleasure to thank Dr. Leon Lucy for discussions and Dr. Robert Jastrow for his hospitality at the Institute for Space Studies.

REFERENCES

Allen, C. W. 1963, Astrophysical Quantities (London: Athlone Press).

Arp, H. 1958, Handbuch der Physik, ed. S. Flügge (Berlin: Springer-Verlag), 51, 75.

Böhm-Vitense, E. 1963, Pub. A. S. P., 75, 154.

Chandrasekhar, S. 1939, An Introduction to the Study of Stellar Structure (Chicago: University of Chicago Press).

Chandrasekhar, S., and Lebovitz, N. R. 1962, Ap. J., 136, 1105.

Crawford, D., Limber, D. N., Mendoza, E., Schulte, D., Steinman, H., and Swihart, T. 1955, Ap. J., 121, 24.

Gurm, H. S. 1963, M. N., 126, 419.

Harris, D. L. 1963, Basic Astronomical Data, ed. K. Aa. Strand (Chicago: University of Chicago Press), p. 263.

Hayashi, C., and Cameron, R. C. 1962, Ap. J., 136, 166.

Henyey, L. G., LeLevier, R., and Levée, R. D. 1959, Ap. J., 129, 2.

Kushwaha, R. S., 1957, Ap. J., 125, 242.

Ledoux, P. 1939, Ap. Norvegica, 3, 193.

———. 1951, Ap. J., 114, 373.

———. 1958, ibid., 128, 336.

Ledoux, P., and Walraven, Th. 1958, Handbuch der Physik, ed. S. Flügge (Berlin: Springer-Verlag), 51, 353.

McNamara, D. H., and Hansen, K. 1961, Ap. J., 134, 207.

Oke, J. B. 1954, Ap. J., 120, 22.

Reddish, V. C., and Sweet, P. A. 1960, Modèles d'étoiles et évolution stellaire (extrait des Mém. Soc. R. Sci. Liège, 5th Ser., Vol. 3), p. 263.

Sahade, J., ed. 1962, Symposium on Stellar Evolution (La Plata,

Sakashita, S., Ôno, Y., and Hayashi, C. 1959, Prog. Theoret. Phys. (Kyoto), 21, 315.

Schmalberger, D. C. 1960, Ap. J., 132, 591.

Schwarzschild, M. 1941, Ap. J., 94, 245.

———————. 1958, Structure and Evolution of the Stars (Princeton, N. J.: Princeton University Press).

Schwarzschild, M., and Härm, R. 1959, Ap. J., 129, 637.

Smith, H. J. 1955, dissertation, Harvard University.

Steinitz, R. 1964, Studies on Magnetic Stars (Proefschrift, Leiden).

Stothers, R. 1963, Ap. J., 138, 1074, "Paper I".

———————. 1964, ibid., 140, in press, "Paper II".

Stothers, R , and Schwarzschild, M. 1961, Ap. J., 133, 343.

Struve, O. 1955a, Pub. A. S. P., 67, 29.

———————. 1955b, ibid., 67, 135.

van Hoof, A. 1961, Zs. f. Ap., 53, 106, 124.

———————. 1962a, ibid., 54, 244.

———————. 1962b, ibid., 54, 255.

———————. 1962c, ibid., 56, 15.

———————. 1962d, ibid., 56, 27.

———————. 1962e, Kleine Veröff. d. Remeis-Sternwarte Bamberg, No. 34, p. 68.

———————. 1963, Zs. f. Ap., 56, 141.

Westerlund, B. 1961, Uppsala Ann., 5, No. 1.

Westerlund, B. E., and Smith, L. F. 1963, preprint.

Table 1

Evolutionary Models during Hydrogen-Burning

	15 $M_\odot$						20 $M_\odot$					
Model	0	1	2	3	4	5	0	1	2	3	4	5
log C	-3.397	-3.300	-3.200	-3.100	-3.075	-3.067	-3.452	-3.400	-3.300	-3.200	-3.150	-3.140
λ	.....	0.822	0.969	1.108	1.185	1.21	.....	0.872	0.976	1.155	1.231	1.28
log q_1	.....	-0.331	-0.316	-0.299	-0.294	-0.293	.....	-0.282	-0.261	-0.239	-0.227	-0.225
log $q_{2,3}$	.....	-0.344	-0.347	-0.352	-0.354	-0.354	.....	-0.292	-0.296	-0.305	-0.311	-0.313
log q_4	-0.343	-0.414	-0.505	-0.622	-0.660	-0.673	-0.291	-0.327	-0.404	-0.499	-0.563	-0.578
X_2	.....	0.700	0.699	0.695	0.694	0.693	.....	0.700	0.698	0.690	0.683	0.681
X_3	.....	0.697	0.691	0.679	0.674	0.674	.....	0.699	0.688	0.666	0.650	0.645
X_4	0.700	0.537	0.331	0.093	0.025	0.004	0.700	0.611	0.419	0.193	0.062	0.035
β_c	0.887	0.859	0.819	0.760	0.740	0.733	0.843	0.824	0.781	0.719	0.678	0.669
log T_c	7.521	7.537	7.558	7.603	7.639	7.686	7.539	7.547	7.565	7.597	7.631	7.647
log ρ_c	0.737	0.730	0.752	0.861	0.966	1.110	0.622	0.620	0.629	0.693	0.788	0.836
log $(L/L_\odot)$	4.400	4.498	4.598	4.698	4.723	4.731	4.720	4.772	4.872	4.972	5.022	5.032
log $(R/R_\odot)$	0.630	0.693	0.780	0.899	0.923	0.897	0.710	0.742	0.819	0.928	1.001	1.013
log T_e	4.548	4.541	4.523	4.488	4.482	4.498	4.589	4.586	4.572	4.542	4.518	4.515
$\bar{X}$	0.700	0.632	0.560	0.494	0.479	0.474	0.700	0.656	0.573	0.493	0.455	0.447
τ (10^6 years)	0.00	3.55	6.52	8.68	9.12	9.25	0.00	1.52	3.96	5.83	6.58	6.72

Table 3

Interpolated Model Characteristics for the Phase of Equal Calculated and Observed Period Ratios

	15 $M_\odot$	20 $M_\odot$	30 $M_\odot$	Standard
$\log(L/L_\odot)$	4.57	4.94	5.40	....
$\log T_e$	4.53	4.55	4.56	....
q_4	0.33	0.34	0.35	....
$\tau(10^6$ years)	5.6	5.2	4.6	....
$\log(R/R_\odot)$	0.75	0.89	1.10	....
$\rho_c/\bar{\rho}$	45:	70:	200:	54.2
X_c	0.39	0.27	0.1	....
ω_o^2	6.6	6.5	6.4	9.26
Π_o (hours)	3.7	5.2	9	....
Q_o (days)	0.045	0.046	0.046	0.038
Π_1/Π_o	0.675	0.678	0.68	0.738

Table 4

Observed Period Ratios in β Cephei Stars

	θ Oph	ν Eri	β Cep	β Cru	β CMa
Π_o (hours)	3.37	4.17	4.57	5.67	6.03
Π_1/Π_o	0.659:	0.675	0.674	0.678	0.679
Π_2/Π_o	0.494	0.505	0.506	0.509	0.509
Π_3/Π_o	0.395:	0.404	0.404	0.408:	0.407
Π_4/Π_o	0.330:	0.336	0.336	0.340:	0.337
Π_2/Π_1	0.750:	0.748	0.751	0.751	0.750
Π_3/Π_1	0.599:	0.599	0.599	0.602:	0.599
Π_4/Π_1	0.501:	0.498	0.499	0.501:	0.496
van Hoof	1962b	1961	1962c	1962a	1962d

FIGURE CAPTIONS

Fig. 1. - Normalized pulsation amplitude as a function of radius fraction for model 4 of 15 $M_\odot$. Solutions are labeled with the mode number. Roman numerals designate the stellar zones (Paper I), which are marked off by vertical lines.

Fig. 2. - Effective polytropic index as a function of mass fraction for the standard model and for models 0 and 4 of 15 $M_\odot$. A dot marks the boundary of the convective core.

Fig. 3. - Theoretical H-R diagram of the upper main sequence, including observational points for the β Cephei stars. Model sequences for 15 - 20 - 30 $M_\odot$ are due to Stothers, and those for 11 - 20 $M_\odot$ to Henyey, LeLevier, and Levée. Crosses mark the interpolated models for equal calculated and observed period ratios.

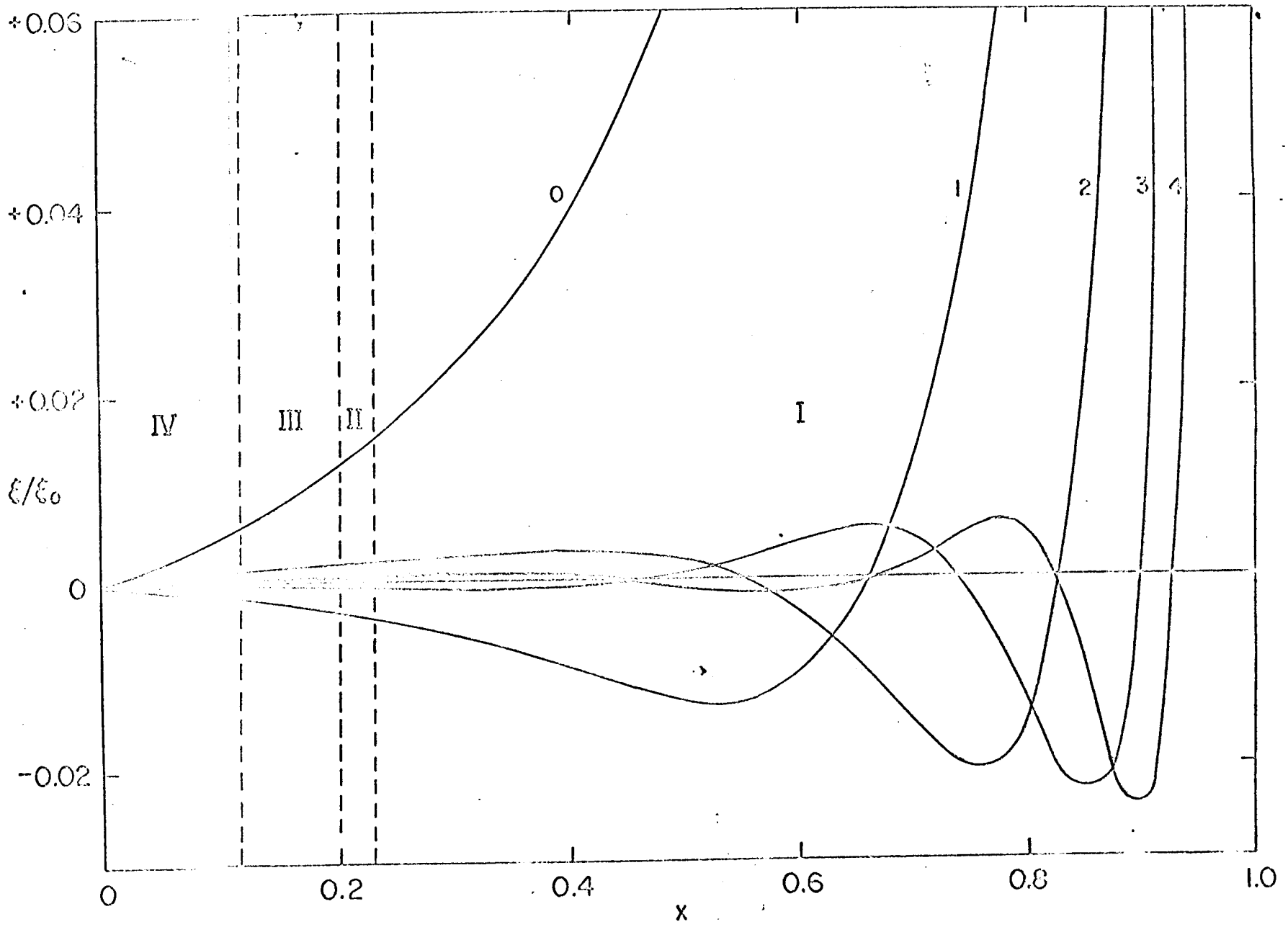
+0.06
+0.04
+0.02
0
-0.02
ε/ε₀
IV
III
II
I
0
1
2
3
4
0
0.2
0.4
0.6
0.8
1.0
x

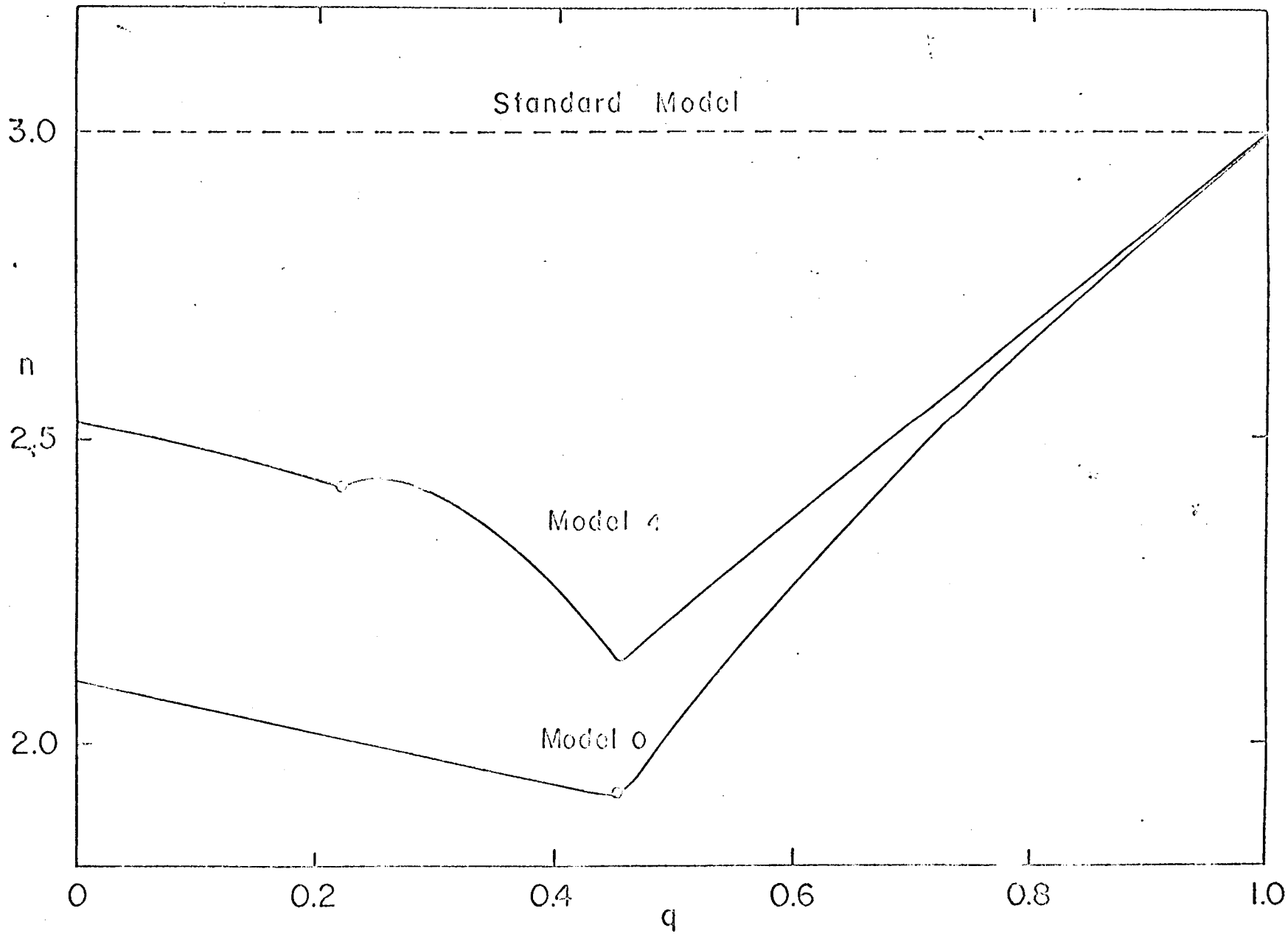
Standard Model
3.0
n
2.5
2.0
Model 4
Model 0
0
0.2
0.4
0.6
0.8
1.0
q

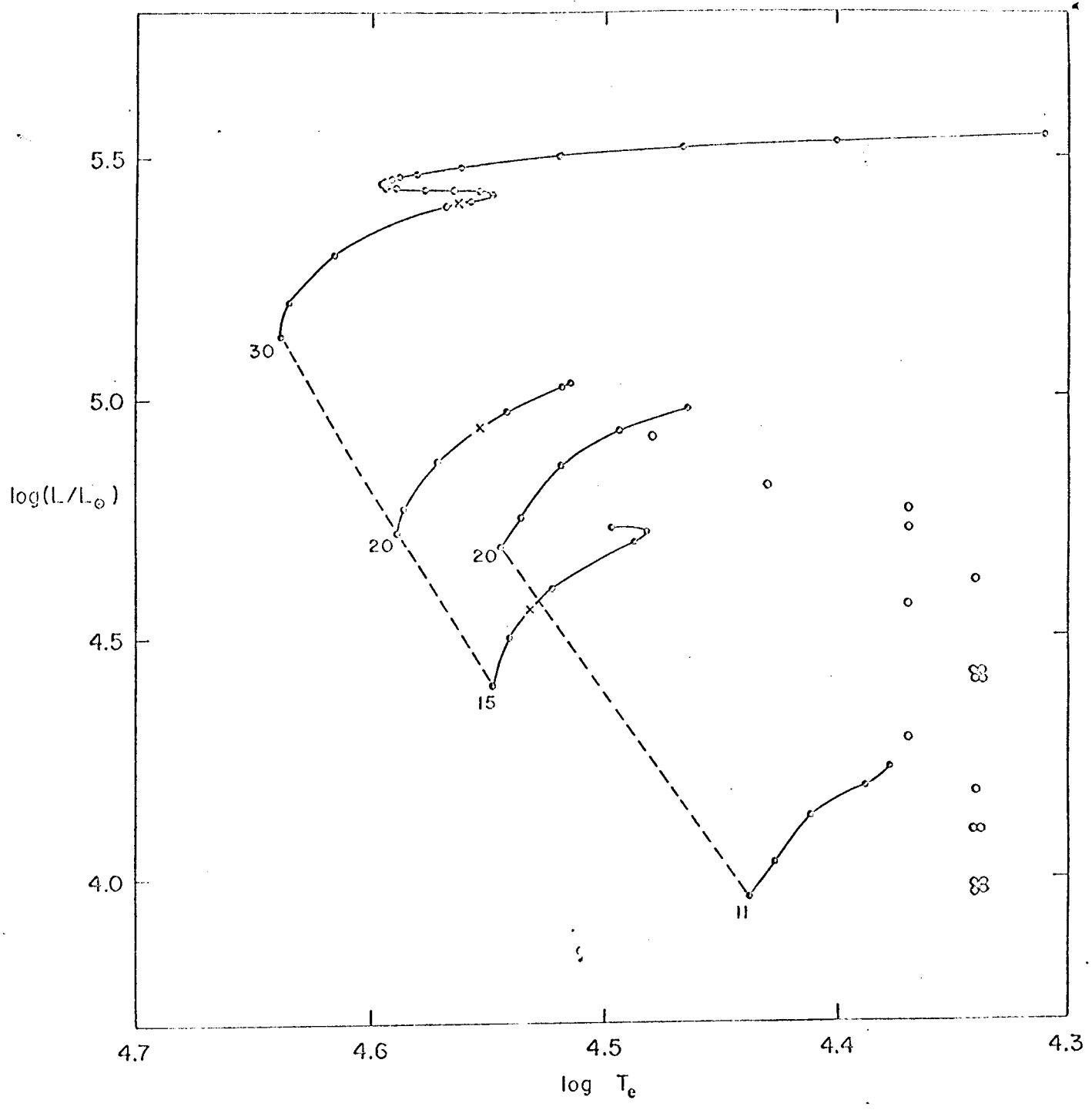
5.5
5.0
4.5
4.0
log(L/L⊙)
30
20
20
15
11
4.7
4.6
4.5
4.4
4.3
log Te

le 2

olutionary Models for Massive Stars

	20 $M_\odot$				30 $M_\odot$					
	2	3	4	5	0	1	2	3	4	5
2	0.819	0.928	1.001	1.013	0.817	0.855	0.943	1.090	1.118	1.143
	43.2	107	221	266	20.3	27.2	52.5	178	239	316
1	0.419	0.193	0.062	0.035	0.700	0.583	0.373	0.112	0.069	0.030
	5.89	6.77	7.19	7.27	3.97	4.37	5.22	6.34	6.49	6.63
	4.33	5.90	7.37	7.64	4.28	4.65	5.76	8.70	9.47	10.2
1	0.048	0.045	0.043	0.043	0.058	0.056	0.051	0.046	0.045	0.045
0	0.654	0.690	0.701	0.703	0.549	0.580	0.633	0.681	0.686	0.690
0	0.486	0.519	0.531	0.533	0.402	0.426	0.469	0.511	0.515	.519
9	0.389	0.416	0.426	0.428	0.319	0.338	0.374	0.409	0.413	.416
9	0.324	0.348	0.357	0.358	0.266	0.281	0.312	0.342	0.345	.348
8	0.744	0.752	0.756	0.757	0.732	0.734	0.740	0.750	0.751	0.753
8	0.594	0.603	0.608	0.609	0.581	0.583	0.590	0.601	0.602	0.603
0	0.496	0.504	0.508	0.509	0.484	0.485	0.492	0.502	0.503	0.504